OXFORD UNIVERSITY PRESS | Brain

Astrogliopathy predominates the earliest stage of corticobasal degeneration pathology

Journal:	*Brain*
Manuscript ID	BRAIN-2016-01078.R2
Manuscript Type:	Original Article
Date Submitted by the Author:	n/a
Complete List of Authors:	Ling, Helen; Reta Lila Weston Institute of Neurological Studies, UCL Institute of Neurology Kovacs, Gabor; Medical University Vienna, Institute of Neurology Vonsattel, Jean Paul; Columbia University Medical Center, Pathology Davey, Karen; University College London Institute of Neurology Mok, Kin Ying; University College London Institute of Neurology Hardy, John; UCL, Molecular Neuroscience Morris, Huw; UCL Institute of Neurology, Warner, Thomas; UCL Institute of Neurology, Clinical Neurosciences Holton, Janice; Institute of Neurology, Queen Square Brain Bank for Neurological Disorders, Neuropathology Revesz, Tamas; Queen Square Brain Bank, Dept of Molecular Neuroscience
Subject category:	Neurodegeneration – cellular and molecular
To search keyword list, use whole or part words followed by an *:	Corticobasal degeneration < MOVEMENT DISORDERS, Tau < NEURODEGENERATION: CELLULAR AND MOLECULAR, Astrocyte < NEURODEGENERATION: CELLULAR AND MOLECULAR, Progressive supranuclear palsy < MOVEMENT DISORDERS, Neurofibrillary tangles < NEURODEGENERATION: CELLULAR AND MOLECULAR

Astrogliopathy predominates the earliest stage of corticobasal degeneration pathology

Authors: Helen Ling[1, 2, 3], Gabor G Kovacs*[4], Jean Paul Vonsattel*[5], Karen Davey[1, 2], Kin Ying Mok[3, 6], John Hardy[3], Huw R Morris[7], Thomas T Warner[1, 2, 3], Janice L Holton[1, 2, 3], Tamas Revesz[1, 2,3]

*These authors contributed equally

Affiliations:

1. Queen Square Brain Bank for Neurological Disorders, UCL Institute of Neurology, University College London, London, UK
2. Reta Lila Weston Institute for Neurological Studies, UCL Institute of Neurology, University College London, London, UK
3. Department of Molecular Neuroscience, UCL Institute of Neurology, University College London, London, UK
4. Institute of Neurology, Medical University of Vienna, Austria
5. Taub Institute for Research on AD and the Aging Brain, Columbia University Medical Center, New York, USA
6. Division of Life Science, Hong Kong University of Science and Technology, Hong Kong SAR, China
7. Department of Clinical Neuroscience, UCL Institute of Neurology, University College London, London, UK

Corresponding author:

Professor Tamas Revesz, Email: t.revesz@ucl.ac.uk; Address: Reta Lila Weston Institute of Neurological Studies, 1 Wakefield Street, UCL Institute of Neurology, London WC1N 1PJ, United Kingdom; Tel.: +44 203 448 4232; Fax: +44 203 448 4286

Running title: Early CBD pathology

Keywords: Corticobasal degeneration; tau; astrocyte; progressive supranuclear palsy; neurofibrillary tangles.

Abbreviations: Aβ: amyloid-β, bvFTD: behavioural variant of frontotemporal dementia, CBD: corticobasal degeneration, CBS: corticobasal syndrome, GM: grey matter, PPA: primary progressive aphasia, PSP: progressive supranuclear palsy, RS: Richardson syndrome, TDP-43: transactive response DNA-binding protein 43 kDa, WM: white matter

Tables: 1

Figures: 7

Supplementary figures: 5

ABSTRACT

Animal models have shown that tau seeding and propagation are strain- and neural network-specific. The study of preclinical cases is valuable to gain insights into early pathological features of corticobasal degeneration and its progression.

Three preclinical corticobasal degeneration cases and six age-matched end-stage corticobasal degeneration cases were included in this study. Tau immunohistochemistry performed in twenty brain regions and quantitative assessment of regional tau load using image analysis were performed. Semi-quantitative grading of tau-positive cellular lesions and neuronal loss in the frontal, parietal and temporal cortices, striatum, substantia nigra and subthalamic nucleus were assessed.

All preclinical cases were clinically asymptomatic but had widespread tau lesions in the typically affected regions in corticobasal degeneration and the pathognomonic astrocytic plaques were the most prominent lesion type in the anterior frontal and striatal regions. Mean total tau load (sum of all regional tau load) of end-stage corticobasal degeneration controls were nine times greater than that of the preclinical cases ($P = 0.04$) and less tau load was found in all regions of the preclinical cases. An anterior-to-posterior tau load ratio in the frontal cortex in preclinical cases was 12-fold greater than in end-stage corticobasal degeneration cases. Relatively greater tau burden in the anterior frontal cortex, striatum and subthalamic nucleus suggest the striatal afferent connection to the dorsolateral prefrontal cortex and basal ganglia circuitry are the earliest neural network connections affected by corticobasal degeneration-related tau pathology. Differential distribution to selective cortical regions in these preclinical cases implies phenotypic presentation may be predetermined at a very early stage of the disease process. Neuronal loss of the substantia nigra was either absent or very mild in the preclinical cases and was moderate to severe in end-stage corticobasal degeneration cases ($P < 0.05$).

Our findings suggest that a threshold of pathological burden in the 'right' anatomical regions needs to be reached before the onset of clinical symptoms. The early prominent astrocytic plaques in relation to trivial neuronal lesions leads one to speculate that corticobasal degeneration may begin as an astrogliopathy at a very early disease stage but neuronal lesion gradually takes over as the predominant lesion type in advanced disease.

INTRODUCTION

Corticobasal degeneration (CBD) is a progressive neurodegenerative tauopathy characterised by the accumulation of hyperphosphorylated 4-repeat tau in the neurons and glia in both cortical and subcortical regions(Dickson *et al.*, 2002). Astrocytic plaques are pathognomonic for CBD and are numerous in affected cerebral cortical areas and the striatum. Neuropil threads are usually numerous and, along with neurofibrillary tangles, pretangles and oligodendroglial coiled bodies, are widespread but are generally greater in the cortex and basal ganglia than in the brainstem and cerebellum. αB-crystallin-immunoreactive ballooned neurons are common and support the diagnosis of CBD (Fig. 1). They are observed in the cortical regions, more frequently in the superior frontal gyrus. In affected cortical areas, spongiosis is usually most evident in layers two and three and astrogliosis is prominent at the grey-white matter junction with myelin loss and microgliosis in the cerebral white matter. Loss of pigmented cells and gliosis in the substantia nigra are consistent findings.

Similar to progressive supranuclear palsy (PSP)(Ling *et al.*, 2013), which is also a 4-repeat tauopathy, the distribution of neuronal loss and severity of tau pathology in CBD closely correlate with its heterogeneous clinical presentations(Kouri *et al.*, 2011). Corticobasal syndrome (CBS) is the classic presentation with asymmetrical focal cortical signs including limb apraxia, dystonia and akinetic-rigidity (CBD-CBS)(Rebeiz *et al.*, 1967, 1968). Clinicopathological studies have shown that other phenotypes such as Richardson syndrome (CBD-RS; i.e. a PSP-like syndrome) and frontotemporal dementia (FTD) including behavior variant FTD (CBD-bvFTD) or primary progressive aphasia (CBD-PPA) may be more common than CBS, as a clinical manifestation of CBD pathology(Ling *et al.*, 2010). Clinical criteria have been proposed to capture the different clinical phenotypes caused by underlying CBD pathology(Armstrong *et al.*, 2013). MRI studies showed that cortical atrophy in CBD-CBS was most marked in the posterior half of the frontal lobe with the superior frontal gyrus being often more affected than the middle and inferior frontal gyri(Whitwell *et al.*, 2010). In such cases, the pre- and postcentral regions are also affected to varying degrees, but the temporal and occipital lobes are usually spared. In CBD-bvFTD and CBD-PPA, atrophy is more severe in the frontal and temporal lobes(Whitwell and Josephs, 2012).

Hierarchical staging schemes depicting stereotypic spatiotemporal progression of neuronal vulnerability as the disease progresses have been proposed for conditions with tau pathology

such as Alzheimer's disease(Braak *et al.*, 2006), argyrophilic grain disease(Saito *et al.*, 2004), Pick's disease(Irwin *et al.*, 2016) and chronic traumatic encephalopathy(McKee *et al.*, 2013) as well as for Parkinson's disease(Braak *et al.*, 2003), a synucleinopathy, bvFTD(Brettschneider *et al.*, 2014) and amyotrophic lateral sclerosis(Brettschneider *et al.*, 2013) with phosphorylated 43-kDa TAR DNA-binding protein (TDP-43) pathology. Animal models and functional magnetic resonance imaging studies have suggested that the progression of tau pathology in conditions such as Alzheimer's disease, CBD and PSP are strain- and neural network-specific(Clavaguera *et al.*, 2009; Clavaguera *et al.*, 2013; Niethammer *et al.*, 2014; Piattella *et al.*, 2015; Ahmed *et al.*, 2016). In recent years, the concepts of tau seeding, cell-to-cell and region-to-region 'spread' of tau pathology, analogous to the prion-like conformational templating mechanism and supported by experimental data and pathological observations, have been proposed as the mechanism responsible for the progression in these neurodegenerative conditions(Lewis and Dickson, 2016). The study of preclinical cases provides a unique resource to detect early pathological changes of the neurodegenerative condition. Similar concepts have been proposed in incidental Lewy body disease representing either preclinical Parkinson's disease(Dickson *et al.*, 2008) or dementia with Lewy bodies(Frigerio *et al.*, 2011) and in preclinical Alzheimer's disease(Braak *et al.*, 2011). In CBD, the regions affected early by tau pathology and its subsequent spatiotemporal progression are not known. This study quantitatively analysed the CBD pathological changes in 3 preclinical cases and compared them with end-stage CBD cases with an aim to determine the early pathological features of CBD.

MATERIALS AND METHODS

Case material

As part of a large-scale study on CBD, we collected 130 CBD cases from 12 UK, European and USA centres. Of these, three cases were identified to have preclinical CBD pathology. These cases had the pathological hallmarks of CBD but were clinically asymptomatic. Six age-matched end-stage CBD cases were selected as controls, three of which had the clinical phenotype of CBS (CBD-CBS) and three clinically presented with Richardson syndrome (CBD-RS). All six end-stage CBD cases had clinically advanced disease following

progressive deterioration and died of end-stage disease; their post-mortem findings fulfilled the pathological diagnostic criteria for CBD(Dickson *et al.*, 2002). End-stage CBD cases with minimal concurrent Alzheimer-type and vascular pathologies were selected. Histological examination and diagnostic confirmation were established in all cases by a neuropathologist (TR). This Queen Square Brain Bank study was approved by a London Multi-Centre Research Ethics Committee and tissue is stored for research under a license from the Human Tissue Authority. Clinical information was extracted from all available medical records by a neurologist (HL).

Neuropathological methods

For Cases 2 and 3, tissue slides were requested from Taub Institute for Research on Alzheimer's disease and the Aging Brain, Columbia University Medical Center, New York, USA and the Institute of Neurology, Medical University of Vienna, Austria, respectively. For Case 1 (from Queen Square Brain Bank) and all six end-stage CBD cases, the brains were divided in the mid-sagittal plane. One half, chosen randomly, was frozen, and the other half was immersed and fixed in 10% buffered formalin for 3 weeks before neuropathological examination. Tissue blocks were taken using the Queen Square Brain Bank protocol. Eight-µm-thick histological sections were stained using routine histological (haematoxylin and eosin, H&E) and silver staining (Gallyas)(Braak *et al.*, 2011) techniques. Immunohistochemistry with antibodies to the following proteins: tau (AT8 clone; Thermo scientific MN1020; 1:600), 3-repeat tau (Gift from Dr Rohan de Silva; 1:150,) and 4-repeat tau (Gift from Dr Rohan de Silva; 1:750), AT100 (Thermo Scientific MN1060; 1:200), αB-crystallin (Leica Biosystems NCL-ABCrys-512, clone G2JF; 1:300), amyloid-β (Aβ; Biosource international, Camarillo, CA, Mouse Dako, clone 6F/3D; 1:100), transactive response DNA-binding protein 43 kDa (TDP-43; monoclonal; clone 2E2-D3; 1:2000), p62 (BD Transduction Labs, Oxford, UK; 1:200) and α-synuclein (Novocastra, Milton Keynes, UK; 1:50) was performed using a standard avidin-biotin method. The following additional pathologies were systematically assessed: p62-positive neuronal cytoplasmic inclusions seen in cases with *C9orf72* mutation, cerebral amyloid angiopathy, argyrophilic grain disease(Saito *et al.*, 2004) and TDP-43 proteinopathy. For determining the level of Alzheimer's disease neuropathological change, ABC score were established according to the National Institute on Aging-Alzheimer's Association (NIA-AA) Guidelines(Hyman *et al.*, 2012).

Quantitative analysis of tau load

Twenty brain regions which are known to be affected in CBD and whose involvement is predicted to contribute to the clinical features were selected: the anterior frontal cortex (Brodmann area 9 or prefrontal cortex) grey matter and white matter, posterior frontal cortex (Brodmann area 4 or primary motor cortex) grey and white matter, middle temporal gyrus (Brodmann area 21) grey and white matter, superior parietal lobule (Brodmann area 7) grey and white matter, hippocampal formation (CA1-4, granular cell layer of the dentate gyrus, subiculum), amygdala, caudate, putamen, globus pallidus, subthalamic nucleus, midbrain tectum and tegmentum, pontine tegmentum and base, cerebellar dentate nucleus and white matter. The posterior frontal cortex and the subthalamic nucleus were not available in Case 2.

Histological AT8-stained slides were digitized on a LEICA SCN400F scanner (LEICA Milton Keynes, UK) with a x20 objective. Slides were viewed and managed on LEICA Slidepath (LEICA Milton Keynes, UK). Brain regions of interest were manually selected and digitally outlined (HL and KD) using Definiens Developer 2.3 (Definiens, Munich, Germany). Threshold was adjusted to capture the two-dimensional area of all AT8-stained lesions (brown) and the same threshold setting was used for all cases. For each selected region, the 'areal fraction', defined by the ratio of the total area occupied by the tau-immunoreactive lesions and the entire area of interest, was computed by Definiens Developer 2.3 (Definiens, Munich, Germany). 'Regional' tau load for each brain region was expressed as percentage (areal fraction x 100%)(Gundersen *et al.*, 1988). 'Total' tau load was the sum of tau load in all 20 regions. 'Cortical' tau load was the sum of tau load of grey and white matter of the anterior frontal, posterior frontal, temporal and parietal regions. 'Basal ganglia' tau load was the sum of tau load of the caudate, putamen, globus pallidus and subthalamic nucleus.

Quantitative analysis of cellular lesion types

Tau-positive cellular lesions including neuronal lesions (neurofibrillary tangles and pretangles), astrocytic plaques and coiled bodies were manually counted (by HL), while neuropil threads were graded semi-quantitatively using a four-tier scale (0-3 with grade 0 = absent to grade 3 = severe) at x20 objective in 5 random fields (3 random fields in the substantia nigra, subthalamic nucleus and cerebellar dentate nucleus due to their relatively

small regional areas) in selected brain regions. A mean score for each lesion type was generated for each brain region. Semi-quantitative analysis of different cellular lesion types using a four-tier scale was performed in the hippocampal formation.

Neuronal loss in the substantia nigra

Neuronal loss in the substantia nigra was determined using a four-tier semi-quantitative grading system by a neuropathologist (TR): 0-3 with grade 0 = no neuronal loss to grade 3 = most severe neuronal loss. The substantia nigra was divided for the grading assessment into 5 subregions: medial, dorsomedial, dorsolateral, ventrolateral and lateral.

MAPT gene sequencing

DNA was extracted from the frozen brain tissue of the three preclinical CBD cases. Exons 10-13 of the *MAPT* gene were screened through Sanger sequencing for known pathological mutations. MAPT haplotypes were determined through the H1/H2-tagging SNP rs1052553(Pittman *et al.*, 2005).

Statistical analysis

The SPSS 24.0 statistical package (IBM Corporation, New York, USA) was used. Log transformation was performed to normalize data where indicated including regional, total, cortical and basal ganglia tau load. Student's *t*-test and ANOVA were used to compare mean tau load (Log10), and continuous demographic data. Pearson χ^2 test was used to compare the neuronal-to-astrocytic lesion ratios between the two CBD groups. Multiple regression analysis was performed to study which of the cellular lesion types best correlate with tau load in the cortical regions. *P* value of 0.05 was used. Corrections for multiple comparisons of mean regional tau load were performed using a *P* value of 0.0031 (16 regions of interest). However, due to the small sample size of the preclinical cases, results without adjustment for multiple comparisons are also reported and discussed.

RESULTS

Overview

The 3 preclinical CBD cases (Cases 1-3) were clinically asymptomatic for any progressive neurodegenerative disorder and incidental findings of histological hallmarks of CBD including astrocytic plaques (Fig. 1) and a combination of neuronal and glial tau pathologies were identified at post-mortem. Six end-stage CBD cases were selected as age-matched controls and were made up of two different clinical phenotypes, CBD-CBS (N = 3) and CBD-RS (N = 3).

The mean age at death of the preclinical CBD group was 76.0 years (SD = 13.0), whereas the mean age at death of the six end-stage CBD cases and our large end-stage CBD cohort collected from 12 international centres for an ongoing pathological staging study was 70.2 years (SD = 5.2, vs. preclinical CBD cases: $P = 0.35$) and 70.6 years (N = 109, SD = 7.9, range = 48 to 88 years, vs. preclinical CBD cases: $P = 0.25$), respectively. The mean disease duration from symptom onset to death of the CBD-CBS and CBD-RS groups was 6.7 years and 4.3 years, respectively ($P = 0.07$). The demographic features of these 9 cases were summarized in Table 1.

Case summary

Case 1 (*London, UK*)

This case was included in our published CBD case series(Ling *et al.*, 2010). This man had motor tics since the age of 8 and developed vocal tics in his late teens. He had lifelong anxiety disorder and an obsessive-compulsive personality trait. Four generations of his family had had a history of motor tics. He was followed up with the neuropsychiatrists at the National Hospital for Neurology and Neurosurgery, Queen Square, London, during which he joined the Queen Square Brain Bank donor programme. He died of metastatic carcinoma of the prostate at the age of 63.

Tau immunohistochemistry revealed moderate number of astrocytic plaques in the anterior frontal region. Occasional neurofibrillary tangles, pretangles and neuropil threads were seen mainly in the anterior frontal, entorhinal and transentorhinal cortices. Sparse neuropil threads

were observed in the posterior frontal, parietal and temporal regions. No ballooned neurons were found on αB-crystallin immunohistochemistry (Fig. 1). In the striatum, there were frequent astrocytic plaques, moderate threads, few neurofibrillary tangles and occasional oligodendroglial coiled bodes. In the putamen, tau pathologies were more prominent in the medial than lateral region. Moderate neuropil threads and few neurofibrillary tangles were seen in the amygdala, substantia nigra and subthalamic nucleus. A few neuropil threads were observed in the locus coeruleus. Scattered neurofibrillary tangles and threads were observed in the midbrain tectum and tegmentum, pontine tegmentum and cerebellar dentate nucleus. Astrocytic plaques, neurofibrillary tangles, pretangles and threads were immunoreactive for 4-repeat tau but not 3-repeat tau. Mild pigment incontinence was seen in the substantia nigra. The volume of the subthalamic nucleus, locus coeruleus and cerebellar dentate nucleus was well-preserved.

Case 2 (*New York, USA*)

This man was a participant in the Washington Heights and Inwood and Columbia Aging Project and was clinically referred to as a 'healthy control' brain donor at the New York Brain Bank. His last scheduled neurological assessment which took place a few months prior to his death at age 89 concluded 'normal cognition' and neurological examination was normal.

Tau immunohistochemistry revealed moderate number of astrocytic plaques in the frontal cortex and striatum and, to a lesser extent, in the temporal region and rarely in the parietal region. There were also scattered neurofibrillary tangles and neuropil threads in these cortical regions as well as in the hippocampal formation, amygdala, striatum, globus pallidus, midbrain tectum, tegmentum, substantia nigra, locus coeruleus and pontine tegmentum. Rarely, a couple of scattered coiled bodies were observed in the cortical regions. These tau-lesions were immunoreactive for 4-repeat tau but not for 3-repeat tau. No ballooned neurons were found on αB-crystallin immunohistochemistry. There was no evidence of cell loss in the cortices, substantia nigra, locus coeruleus, subthalamic nucleus and dentate nucleus.

Case 3 (*Vienna, Austria*)

The clinical and pathological features of this case were described in a case report(Milenkovic and Kovacs, 2013). In brief, this woman had polycystic kidney disease and chronic renal

insufficiency. Shortly following renal transplantation, she developed acute graft rejection and was treated with immunosuppressants, but eventually succumbed to septic shock and multiple organ failure at the age of 76.

Mild neuronal loss and gliosis were observed in the parietal, temporal and entorhinal cortices and substantia nigra. Moderate gliosis was observed in the caudate. Occasional ballooned neurons immunoreactive for αB-crystallin were found only in the anterior cingulate cortex. Mild to moderate tau pathologies including astrocytic plaques, neurofibrillary tangles, pretangles, threads and occasional coiled bodies were seen in the frontal cortex, striatum, substantia nigra, hippocampus, amygdala and, to a lesser extent, parietal, temporal and entorhinal cortices, globus pallidus and subthalamic nucleus. Few neuropil threads were detected in the locus coeruleus. Argyrophilic grains (Stage II) immunoreactive for 4-repeat tau and p62 antibodies were observed in the hippocampal formation(Saito *et al.*, 2004). Mild pigment incontinence was seen in the substantia nigra. There was no evidence of neuronal loss in the frontal cortex, subthalamic nucleus and locus coeruleus.

Quantitative analysis of tau load

Regional tau load

The mean regional tau load of the preclinical CBD group was less than that of the end-stage CBD group with statistically significant difference identified in 16 selected regions ($P < 0.05$). For the remaining 4 selected regions, there was borderline significance in the anterior frontal grey matter, parietal white matter and putamen, and no statistical significance in the amygdala ($P = 0.15$)(Fig. 2 & Fig. 3). After adjusting for multiple comparisons, significant difference in mean regional tau load between the preclinical and end-stage groups was identified in the following regions: posterior frontal grey and white matter, temporal grey matter, caudate nucleus, midbrain tectum, and pontine tegmentum. The regional tau load data of selected brain regions of the preclinical CBD cases are illustrated in Supplementary Fig. 1.

Frontal tau load distribution

Of all the cortical regions, the most abundant tau load in the preclinical CBD group was identified in the frontal cortex. Within the frontal cortex, the predominant tau load was observed in the anterior frontal region and tau lesions in the posterior frontal region were

very sparse (Fig. 4). This finding was in contrast with the severe tau load in the posterior frontal region usually found in end-stage CBD-CBS cases. The mean anterior-to-posterior frontal tau load ratio (including both grey and white matter) of the preclinical CBD group was 16.04 and that of the end-stage CBD group was 1.36. Thus, the anterior-posterior gradient of tau distribution in the frontal region of the preclinical CBD group was almost 12 folds greater than that of the end-stage CBD group.

Total, cortical and basal ganglia tau load

The total ($P = 0.04$) and basal ganglia ($P = 0.001$) tau load of the preclinical CBD group were significantly less than those of the end-stage CBD group. Although cortical tau load of the preclinical CBD group was numerically less than that of the end-stage CBD group, there was no significant difference statistically ($P = 0.19$)(Supplementary Fig. 2).

Cellular lesion types

Overview

The distribution and severity of different tau lesion types based upon quantitative analysis are illustrated in Fig. 5. In the preclinical cases, an anterior-posterior gradient in the distribution of all cellular lesion types could be observed in the frontal cortex with these lesions being mainly restricted to the anterior frontal region rather than the posterior frontal region.

Neuronal lesions and neuropil threads

In end-stage CBD, neuronal lesions (e.g. neurofibrillary tangles and pretangles) were most prominent in the frontal and parietal cortices, amygdala, caudate, subthalamic nucleus and pontine tegmentum; while in preclinical CBD, neuronal lesions were mainly found, to a lesser extent than in the end-stage cases, in the anterior frontal and parietal regions, amygdala and the basal ganglia (Fig. 5). In end-stage CBD, severe neuropil thread pathology was observed in the frontal region, basal ganglia, midbrain tectum, whereas in the preclinical cases, mild thread pathology was found in the frontal cortex, amygdala and basal ganglia and was almost absent in other regions with scattered neuropil threads occasionally observed in the temporal and parietal cortices and cerebellar white matter.

Astrocytic plaques

In end-stage CBD cases, moderate numbers of astrocytic plaques were observed in the frontal, parietal and temporal cortices, amygdala and striatum. In the preclinical cases, astrocytic plaques were most abundant in the striatum, and were observed in mild to moderate density in the anterior frontal, parietal and temporal cortices. astrocytic plaques were uncommon in the brainstem and cerebellum in both groups.

Coiled bodies

In our end-stage CBD cases, oligodendroglial coiled bodies were in general less common than other lesion types and were occasionally observed the cortical white matter, lentiform nucleus and brainstem, whereas in preclinical CBD, very occasional coiled bodies were observed in the anterior frontal region and lentiform nucleus.

Tau lesion types in the cortical regions

In the end-stage CBD cases, neuronal lesions in the cortical regions were at least 4 times more abundant than astrocytic plaques; while the proportion of these two lesion types was similar in the preclinical CBD cases (Supplementary Fig. 3). The average ratio of neuronal lesions to astrocytic plaques in the four cortical regions (anterior and posterior frontal, parietal and temporal cortical grey matter) was 0.91 in the preclinical CBD group and 4.20 in the end-stage CBD group ($P < 0.001$; χ^2 test).

Multiple regression analysis was performed to investigate which of the cellular lesion type best correlates with regional tau load in cortical grey matter (Supplementary Fig. 4). In the preclinical CBD cases, there was a significant correlation between neuronal lesions and regional tau load ($P = 0.002$, $R^2 = 0.98$), while in the end-stage CBD cases, neuropil threads ($P < 0.001$) and neuronal lesions ($P = 0.056$, borderline significance) significantly correlated with regional tau load ($R^2 = 0.87$). Other lesion types such as astrocytic plaques and coiled bodies did not correlate with the regional tau load in either CBD group.

Tau lesion types in the hippocampal formation

The distribution and severity of neuronal and thread pathologies in the hippocampal formation are illustrated in Supplementary Fig. 5. Tau lesions in the hippocampal subregions were very mild in preclinical Cases 1 and 2. In preclinical Case 3 and most of the end-stage CBD cases, severe neuronal and thread pathologies were observed in CA1 and the granular cell layer even in cases with no or minimal Alzheimer's disease-related changes and absence of argyrophilic grains (e.g. Cases 4-6). In preclinical CBD cases, mild astrocytic plaques were observed in CA1, subiculum (Cases 1 and 2), and entorhinal cortex (Cases 1 and 3). Astrocytic plaques were observed in the entorhinal cortex of three of the six end-stage CBD cases, ranging from mild (Cases 4 and 8) to severe (Case 9).

AT100 immunohistochemistry

For both the preclinical and end-stage CBD cases, the tau-positive lesions (neurofibrillary tangles, pretangles, neuropil threads, astrocytic plaques and coiled bodies) were also immunoreactive with antibody AT100 (Fig. 1). This finding indicated that disease-associated tau in all lesion types observed in the preclinical cases was phosphorylated at serine 212 and threonine 214 and was in advanced stage of the aggregation process and formed filaments i.e. tau was in the same conformation as the tau lesions in end-stage cases (Clavaguera *et al.*, 2009).

Cell loss in substantia nigra

Semi-quantitative assessment of cell loss using a four-tier rating scale in five substantia nigra subregions showed that the cell loss was either absent or very mild in the preclinical cases, while in the end-stage cases, the nigral cell loss ranged from moderate to severe (medial, dorsomedial and ventromedial subregions: $P = 0.03$, χ^2 test), with the ventrolateral subregion being most severely and consistently affected in all six end-stage cases ($P = 0.01$; χ^2 test); one exception was in the dorsolateral subregion ($P = 0.06$, borderline significance; χ^2 test) where cell loss was found to be mild in a CBD-CBS case (Case 4)(Fig. 6).

Secondary pathologies

Secondary pathologies in preclinical and end-stage cases are summarized in Table 1. Argyrophilic grains were observed in one preclinical case (Case 3, Vienna). Mild cortical Aβ

pathology was observed in another preclinical case (Thal phase 1, Case 2, New York, age of death: 89 years). TDP-43, α-synuclein, vascular and cerebral amyloid angiopathy pathologies were not identified in any of the preclinical cases.

MAPT gene sequencing

Sanger sequencing of *MAPT* gene for any known pathological mutations in exons 10-13 were negative in all three preclinical CBD cases. Preclinical Cases 1 and 3 had H1/H1 and Case 2 had H1/H2 *MAPT* haplotypes.

DISCUSSION

We described the histological features of three clinically asymptomatic cases with CBD-tau lesions in both neurons and glia. These lesions were immunoreactive with the AT8, AT100 and anti-4-repeat tau antibodies but not with the antibody to 3-repeat tau. Astrocytic plaques with Gallyas-positive and tau-imunoreactive annular clusters of short processes were seen, most prominently in the striatum followed by the anterior frontal and parietal regions. The severity of neuronal lesions and neuropil threads followed a rostro-caudal descending gradient from the forebrain to the hindbrain structures but the overall tau burden in the preclinical cases was significantly less than the end-stage CBD cases. Cortical neuronal loss, spongiosis, ballooned neurons, thinning of the corpus callosum, nigral cell loss, all of which are considered to be characteristic features of end-stage CBD, were consistently observed in all six of our end-stage CBD cases, but were either absent or minimal in the three preclinical cases. We interpreted these histological findings as early CBD pathology and the lack of clinical symptoms was due to subthreshold pathology.

The distribution and severity of neuronal loss and tau pathology are closely associated with the clinical syndrome in CBD as in other neurodegenerative conditions (Boxer *et al.*, 2006; Whitwell *et al.*, 2010; Ling *et al.*, 2013). The lack of significant neuronal loss in the cortex, substantia nigra and less total tau load in our preclinical CBD cases when compared with end-stage CBD cases suggest that a threshold of pathological burden in the 'right' anatomical regions needs to be reached for the onset of clinical symptoms. Despite the relatively smaller number of tau lesions, the tau pathology in preclinical cases is widespread and shows a

topographical distribution that is overall similar to that observed in end-stage cases. As the total tau load of Case 3 was four- and five-fold greater than Cases 1 and 2, it is reasonable to assume that Cases 1 and 2 are at an earlier stage of the pathological process than Case 3.

In Case 1, cortical pathology was very mild and was mainly observed in the anterior frontal region, followed by the posterior frontal region, relatively dense tau pathology was also found in the striatum and subthalamic nucleus. In Case 2, tau pathology was similarly distributed in the frontal and temporal grey and white matter. In Case 3, predominant cortical tau pathology was observed in the anterior frontal and parietal regions as well as in the hippocampus, amygdala and caudate with moderate gliosis in the caudate. In a quantitative study comparing the tau distribution of CBD-CBS and CBD-RS, Kouri et al showed that CBD-CBS cases had significantly greater tau burden in the primary motor and somatosensory cortices of both grey matter and white matter and putamen than in CBD-RS cases and that tau burden in the anterior frontal cortex (superior frontal gyrus) was the same in both CBD phenotypes. Phenotypic presentation of CBD is probably predetermined at a very early stage as seen in our preclinical cases. If these individuals had lived for longer and the disease process were allowed to evolve, Case 2 may have developed an FTD syndrome based on the early predominant tau distribution in the frontal and temporal regions, while Cases 1 and 3 may have had the classic CBS phenotype in view of the early frontal and striatal involvement. Similar to most brain bank protocols, only one brain hemisphere of each case was processed for histological studies and was available for this study. In view of the predilection of tau accumulation in different cortical regions early in the disease process, it is possible that interhemispheric asymmetry of pathology is already evident in these preclinical cases(Oide *et al.*, 2002; Boxer *et al.*, 2006; Hassan *et al.*, 2010), but remains at a subthreshold level bilaterally.

In Cases 1 and 3, tau pathology was more prominent in the anterior frontal region (prefrontal cortex) than in the posterior frontal (precentral gyrus involving primary motor cortex). Unfortunately, the posterior frontal region in Case 2 was not available for analysis. A 12-fold greater anterior-to-posterior frontal tau load ratio was found in these preclinical cases when compared with the end-stage group. This anterior-posterior gradient suggests the initial site of tau accumulation in the frontal cortex is likely to be the anterior frontal region, while the

posterior frontal area is involved at a later stage. Symptom onset of CBS probably coincides with the threshold of pathological burden in the primary motor cortex being reached.

The distribution of cellular lesion types differed between the preclinical and end-stage cases. In the anterior frontal cortex, the mean astrocytic plaque count was 2.5 (range: 0 to 10; averaging over 5 random fields at x20 objective) in Cases 1 and 2 with sparse threads and absence of neuronal lesions, while the mean neuronal and astrocytic plaque counts in the anterior frontal cortex of Case 3 were 6 and 4.6, respectively. In end-stage cases, neuronal lesions in the anterior frontal cortex were three times greater than astrocytic plaques (13.6 to 4.1). Likewise, in the striatum, a region with one of the highest mean tau load in both CBD groups, the mean neuronal and astrocytic plaque counts in Cases 1 and 2 were 2.2 and 13.0, and in Case 3, they were 5.4 and 5. In the end-stage CBD cases, neuronal lesions in the striatum were twice as many as astrocytic plaques (7.9: to 3.2). These findings indicate that astrocytic plaques were the predominant lesion type in the anterior frontal cortex and striatum of Cases 1 and 2, which were thought to be at an earlier disease stage than Case 3. It is possible that astrocytic plaques are the earliest tau lesion type that occurs in regions affected early by the CBD pathological process, leading us to speculate that CBD may begin as an astrogliopathy. Based upon the findings in Case 3 and end-stage cases, it appears that as the pathology progresses, neuronal lesions markedly increase in number and eventually overtake astrocytic plaques as the predominant lesion type. Notably, in some end-stage cases, very dense thread pathology observed in the cerebral cortex and some subcortical grey nuclei may mask a proportion of the astrocytic plaques. Josephs et al studied the correlation between disease duration and lesion types in PSP and noted that cases with the most severe neuronal tau pathology had the longest disease duration (Josephs *et al.*, 2006), indicating that neuronal tau pathology, rather than astrogliopathy, is the most abundant cellular lesion type in end-stage PSP, another 4-repeat tauopathy. Multiple regression analysis has identified a correlation between neuronal lesions and regional tau load in the preclinical group. This finding may be explained by the larger tau-immmunoreactive area attributed by neuronal lesions in Case 3.

In end-stage CBD, there is a variable degree of neuronal loss and gliosis in the substantia nigra (Dickson *et al.*, 2002). Neuronal loss in the ventrolateral nigral cell groups correlates with extrapyramidal features in parkinsonism(Fearnley and Lees, 1991); whereas neuronal loss in the medial nigra correlates more with cognitive and frontal behavioural deficits(Rinne

et al., 1989) and were more severely affected in CBD-RS than CBD-CBS(Kouri *et al.*, 2011). This finding was also confirmed by the present study. Our end-stage CBD-RS cases had more severe neuronal loss in the medial ($P = 0.014$) and dorsomedial ($P = 0.014$) tiers when compared with CBD-CBS cases and severe neuronal loss (grade 3 all) was observed in the ventrolateral tier in both phenotypes. Pirker et al reported two post-mortem confirmed CBD cases with mildly reduced tracer uptake in dopamine transporter SPECT scan in early disease stage (1.5 years after symptom onset), and subsequently, the tracer uptake markedly declined later in the disease course (4.5 and 5 years after symptom onset)(Pirker *et al.*, 2015). Our group previously reported a pathologically confirmed CBD case with normal dopamine transporter SPECT tracer uptake more than 4 years into the illness(O'Sullivan *et al.*, 2008). These findings suggest that nigrostriatal degeneration may be a late pathological feature of CBD. In our preclinical cases, tau pathology in the substantia nigra was mild and the cell population in all nigral subregions was either preserved or showed very mild cell loss (range: grade 0 to 0.5 in all subregions of all three preclinical cases), indicating nigral cell loss takes place later in the disease course.

Severe neuronal loss and gliosis in the subthalamic nucleus is a prerequisite for the pathological diagnosis of PSP(Hauw *et al.*, 1994), but it is not a consistent feature in end-stage CBD. Only three of the six end-stage CBD cases showed mild neuronal loss with gliosis in the subthalamic nucleus, while the volume of the remaining three cases was preserved. In the preclinical cases, the subthalamic nucleus has one of the highest tau burden and tau lesions (mild to moderate neurofibrillary tangles, pretangles and neuropil threads), with preserved volume. Neuronal loss of the subthalamic nucleus is a late feature in the CBD disease process, which is likely related to the downstream pathological involvement from the striatum, pars externa of the globus pallidus and substantia nigra within the basal ganglia circuit.

In preclinical Cases 1 and 2, very mild tau lesions were observed in the hippocampal formation. There were more severe neuronal lesions in preclinical Case 3 but they may be attributable to coexisting argyrophilic grain disease pathology. In the fimbria, only very mild thread pathology was observed in Cases 1 and 2 but this was of moderate degree in Case 3. These findings suggest that tau pathology is minimal in the hippocampal formation in very early disease stage. It is likely that as the disease progresses, the hippocampus and fimbria, which is the white matter outflow of the hippocampus forming the fornix, become gradually

affected by tau pathology. Similar findings were observed in the amygdala, of which the regional tau load was very mild in Cases 1 and 2 (regional tau load: Case 1 = 0.51, Case 2 = 0.48) and was much greater in Case 3 where argyrophilic grains were also present (regional tau load = 24.97)(Supplementary Fig. 1). Based on the findings in Cases 1 and 2, tau pathology in the amygdala is probably mild in very early disease stages in the absence of secondary pathology. Mild tau pathology in the amygdala was also observed in an incidental case (Case 1) recently reported by Nishida et al (Nishida *et al.*, 2015).

Only four preclinical CBD cases have been reported in the literature, two of which are included in this series (Cases 1(Ling *et al.*, 2010) and 3(Milenkovic and Kovacs, 2013)). Recently, two preclinical (or early symptomatic cases) along with one clinically symptomatic end-stage CBD-bvFTD case were identified from 887 brains in a forensic autopsy series in Toyama, Japan, over a 6-year period, giving a pathological incidence rate of 0.34%(Nishida *et al.*, 2015). Case 1 of the Japanese report was a 65-year-old man who had died of smoke inhalation at the scene of a house fire. Case 2 was a 77-year-old woman diagnosed with dementia one month prior to death with a mini-mental state examination score of 21 out of 30 points but did not experience any speech or motor impairments. She died of accidental drowning. Both cases had subtle clinical features consistent with early cognitive impairment. Histological examination of both cases revealed widespread tau pathology including neurofibrillary tangles, pretangles, astrocytic plaques in the fontal, parietal and temporal cortices, limbic, basal ganglia and brainstem structures. Ballooned neurons were observed in the frontal, temporal and limbic cortices. There was moderate neuronal loss in the substantia nigra in both cases. Numerous argyrophilic grains were found in the amygdala in Case 2 (Stage II)(Saito *et al.*, 2004; Nishida *et al.*, 2015). The authors concluded that milder overall tau burden, sparse tau pathology in the superficial cortical layers, and the lack of volume loss or gliosis in the cortices, subcortical white matter and the corpus callosum as shown in their two cases were likely to be early histological features of CBD. In addition to these characteristics, our preclinical cases also exhibited much milder thread pathology which was restricted to the anterior frontal white matter and absent in other subcortical white matter, absent or rare ballooned neurons and preserved substantia nigra, suggesting our cases may represent an even earlier stage of CBD pathology when compared to the two cases described by Nishida et al.

While the preclinical cases in the present series represent very early (Cases 1 and 2) and early (Case 3) CBD pathology, the Japanese cases (Cases 1 and 2)(Nishida *et al.*, 2015) most likely illustrate a continuum of early symptomatic CBD pathology. A pathological threshold that coincides with clinical disease onset is probably marked by an overall increase in tau burden especially in strategic brain regions accompanied by cortical spongiosis, nerve cell loss and the appearance of ballooned neurons as well as early nigral neuronal loss (Fig. 7). Future post-mortem studies of symptomatic patients with CBD who have died of other causes prior to reaching end-stage disease, will be of great value to demonstrate intermediate pathology prior to reaching a fully advanced disease stage.

Argyrophilic grains can be observed in over 40% of end-stage CBD cases(Togo *et al.*, 2002). The findings of argyrophilic grains in one of our preclinical cases (Case 3, Vienna) and in another early CBD case (Case 2) in the Japanese series suggest that argyrophilic grains may be a concomitant pathological feature that occurs early in the CBD pathological process. It is possible that these two distinct 4-repeat tauopathies, CBD and argyrophilic grain disease, share common characteristics which are relevant for the pathogenesis of both diseases. Moreover, the occasional ballooned neurons observed in limbic structures in our Case 3 are most likely driven by the coexisting argyrophilic grain disease rather than by the CBD pathological process(Saito *et al.*, 2004).

Preclinical cases of Alzheimer's disease and Lewy body disease are common and their prevalence is much greater than the prevalence of their symptomatic counterparts(Bouras *et al.*, 1994; Beach *et al.*, 2009; Adler *et al.*, 2010). On the other hand, preclinical cases of other neurodegenerative conditions are very rare, only six preclinical PSP(Oshima *et al.*, 2004; Evidente *et al.*, 2011) and two preclinical multiple system atrophy cases(Parkkinen *et al.*, 2007; Fujishiro *et al.*, 2008) have been described in the literature. Evidente et al reported five preclinical PSP cases with frequent pathognomonic tufted astrocytes in the characteristic brain regions(Evidente *et al.*, 2011). An association between H1 haplotype and 4-repeat tauopathies, including PSP and CBD, was previously reported and H1/H1 haplotype was identified in our preclinical Cases 1 and 3(Houlden *et al.*, 2001).

Our Case 1 died at the age of 63, but, notably, Case 2 in the present series died at age 89 and our Case 3 and Case 2 of the Japanese series also died at a relatively old age of 76 and 77,

respectively. Assuming that all five preclinical cases reported in the present and Japanese series had lived longer and that all cases soon went on to develop clinical symptoms, their estimated age at symptom onset (mean = 74) would have been significantly higher than that of the six end-stage CBD cases used as controls in the present study (mean = 64.2, P = 0.07, borderline significance) and that of our large end-stage CBD cohort (N = 109; mean = 64.6 years, P = 0.01). In view of the fact that three of the five available preclinical cases were significantly older, there remains a possibility that some of these cases may represent a heterogeneous subgroup distinct from the typical CBD cases and our findings should be interpreted with cautions. Future studies are required to explore whether some of these older preclinical cases represent a more 'benign' subgroup due to the presence of distinct protective factors (such as H2 allele in our Case 2) or cognitive reserve (Case 2 also had a demanding professional occupation). This notion would be supported by existing findings in other neurodegenerative diseases such as Parkinson's disease and PSP, of which phenotypic subgroups are segregated by age and disease duration (Williams *et al.*, 2005; Halliday *et al.*, 2008).

The study of preclinical CBD cases provides valuable insights into the early regions and lesion type affected by the CBD pathological process. These findings may serve as a basis for *in vivo* tau-imaging studies in patients with early symptoms to predict underlying CBD pathology, as well as the development of other biomarkers and disease-modifying treatments targeting early disease. Although the rarity of these preclinical cases coming to post-mortem makes further clarification of the true nature of these preclinical cases unlikely unless clinico-pathological studies with a very large sample size are conducted, the widespread neuronal and glial tau lesions found in a typical anatomical distribution as observed in end-stage CBD and the presence of pathognomonic astrocytic plaques support our view that these cases represent early CBD and would have eventually evolved to symptomatic CBD.

In summary, the earliest pathological features of CBD deduced from these three preclinical cases are: 1. Overall less tau burden, 2. astrocytic plaques are an early lesion type most prominent in the prefrontal cortex and striatum, 3. Relatively higher tau load in the anterior frontal cortex, striatum and subthalamic nucleus, suggesting striatal afferent connection to the dorsolateral prefrontal cortex and the basal ganglia circuitry may be the earliest neural network connections affected by CBD-tau(Ahmed *et al.*, 2016), 4. Preserved substantia nigra,

and 5. Either absent or minimal cortical neuronal loss, superficial spongiosis and ballooned neurons.

Figure legends

Fig. 1:

Ballooned neurons (a & b; end-stage CBD Case 6) and astrocytic plaques (c-f; preclinical CBD Case 1).

Ballooned neuron is absent in Cases 1 and 2. Occasional ballooned neurons observed in the cingulate cortex in Case 3 are probably associated with the coexisting argyrophilic grain disease rather than CBD pathology. Astrocytic plaque is a prominent histological finding in preclinical CBD cases, especially in the anterior frontal cortex (c-f) and caudate, and is immunoreactive for AT8 (c), AT100 (e) and 4-repeat tau (f), but not 3-repeat tau, and is Gallyas-positive (d). 1 cm scale bar = 10 µm.

Fig. 2:

Mean regional tau load (Log10) of preclinical CBD and end-stage CBD groups in 20 selected brain regions.

Error bars represent one standard error of the mean (SEM). ****P value < 0.001, ***P value: 0.001-0.005, **P value: 0.005-0.01, *P value: 0.01-0.05, #P value: 0.05-0.01 (borderline statistical significance), Student's t-test; AFG: anterior frontal grey matter, AFW: anterior frontal white matter, PFG: posterior frontal grey matter, PFW: posterior frontal white matter, PRG: parietal grey matter, PR: parietal white matter, TMG: temporal grey matter, TMW: temporal white matter, HIP: hippocampus, AMG: amygdala, CAU: caudate, PUT: putamen, GLP: globus pallidus, STN: subthalamic nucleus, MTC: midbrain tectum, MTG: midbrain tegmentum, PTG: pontine tegmentum, PBS: pontine base, CDN: cerebellar dentate nucleus and CWM: cerebellar white matter.

Fig. 3:

Tau immunohistochemistry (AT8) sections of the three preclinical CBD cases (Cases 1-3) and one end-stage CBD-CBS case (Case 4). 1 cm scale bar = 38.5 µm.

Fig. 4:

Anterior and posterior frontal cortex of two preclinical CBD (Cases 1 and 3) and one end-stage CBD-CBS case (Case 6).

The characteristic features of cortical neuronal loss and superficial spongiosis are observed in the end-stage CBD case (c & i) but not in the preclinical CBD cases (a, b & g, h). In the preclinical CBD cases, tau immunohistochemistry (AT8) demonstrates tau lesions, mainly in the form of astrocytic plaques, are more abundant in the anterior frontal cortex (d & e) than in the posterior frontal cortex (j & k). This anterior-posterior gradient is most apparent in Case 1 (d & j), which has a relatively less total tau load and is thought to represent an earlier stage of CBD pathology than Case 3. On the contrary, in the end-stage CBD case, neurofibrillary tangles and neuropil threads are much more frequent than astrocytic plaques and the tau distribution is more severe in the posterior frontal cortex (l) than in the anterior frontal cortex (f). H&E: a-c, g-i; tau immunohistochemistry (AT8): d-f, j-l; 1 cm scale bar = 100µm.

Fig. 5:

Distribution and severity of tau-immunoreactive cellular lesions in preclinical and end-stage CBD groups.

A summary of the tau pathology in three preclinical CBD and six end-stage CBD (3 CBD-CBS and 3 CBD-RS) cases using mean lesion count for neuronal lesions, astrocytic plaques and coiled bodies and a 4-tier semi-quantitative scores for neuropil thread (0 = none, 1 = mild, 2 = moderate, 3 = severe) assessed at x20 objective in five random fields (except for substantia nigra, subthalamic and dentate nuclei where three random fields were used due to small regional areas). The severity of tau pathology is colour-coded with a heat map, with more severely affected areas showing hotter colours (red, orange and yellow) and less affected areas represented by cooler colours (green and blue).

Fig. 6:

H&E sections of the substantia nigra.

The substantia nigra of the three preclinical CBD Cases 1-3 and an 82-year-old healthy control are relatively preserved with a good population of pigmented neurons. Severe loss of

pigmented neurons, gliosis and scaring are observed in the substantia nigra of the end-stage CBD-RS Case 8. 1 cm scale bar = 100 µm.

Fig. 7:

Characteristic features of the pathological progression of CBD.

Acknowledgements

This project is funded by Karin & Sten Mortstedt CBD Solutions. HL presented this work at the British Neuropathological Society Annual Meeting and the European Congress of Neuropathology in 2016. The authors would like to thank all patients and their families for their support of this research; the Institute of Neurology, Medical University of Vienna, Austria and Taub Institute for Research on Alzheimer's disease and aging Brain, Columbia University Medical Centre, New York, USA for their contributions to this project; James Polke and Manuel Bernal-Quiros for their input for MAPT Sanger sequencing; Linda Parsons for tissue preparation; Robert Courtney for immunohistochemistry, and Matt Ellis for technical support.

Funding

This study was funded by Karin & Sten Mortstedt CBD Solutions research grant (Grant code: 512385).

Conflict of interest

HL, KD, KYM, HRM, TTW, JLH, TR have received research grant from Karin & Sten Mortstedt CBD solutions. HL and KD are employed by Reta Lila Weston Institute of Neurological Studies, UCL Institute of Neurology. HRM receives research grants from the Drake Foundation. This research was partly supported by the National Institute for Health Research (NIHR) Queen Square Biomedical Research Unit in Dementia based at University College London Hospitals (UCLH), University College London (UCL). The views expressed are those of the authors and not necessarily those of the NHS, the NIHR or the Department of Health. JLH is supported by the Multiple System Atrophy Trust, Alzheimer's Research UK, CBD Solutions and the Michael J Fox Foundation. Queen Square Brain Bank is supported by Reta Lila Weston Institute for Neurological Studies and the Medical Research Council UK.

Other authors report no conflict of interest.

REFERENCES

Adler CH, Connor DJ, Hentz JG, Sabbagh MN, Caviness JN, Shill HA, *et al.* Incidental Lewy body disease: clinical comparison to a control cohort. Mov Disord 2010; 25(5): 642-6.

Ahmed RM, Devenney EM, Irish M, Ittner A, Naismith S, Ittner LM, *et al.* Neuronal network disintegration: common pathways linking neurodegenerative diseases. J Neurol Neurosurg Psychiatry 2016.

Armstrong MJ, Litvan I, Lang AE, Bak TH, Bhatia KP, Borroni B, *et al.* Criteria for the diagnosis of corticobasal degeneration. Neurology 2013; 80(5): 496-503.

Beach TG, Adler CH, Lue L, Sue LI, Bachalakuri J, Henry-Watson J, *et al.* Unified staging system for Lewy body disorders: correlation with nigrostriatal degeneration, cognitive impairment and motor dysfunction. Acta Neuropathol 2009; 117(6): 613-34.

Bouras C, Hof PR, Giannakopoulos P, Michel JP, Morrison JH. Regional distribution of neurofibrillary tangles and senile plaques in the cerebral cortex of elderly patients: a quantitative evaluation of a one-year autopsy population from a geriatric hospital. Cereb Cortex 1994; 4(2): 138-50.

Boxer AL, Geschwind MD, Belfor N, Gorno-Tempini ML, Schauer GF, Miller BL, *et al.* Patterns of brain atrophy that differentiate corticobasal degeneration syndrome from progressive supranuclear palsy. Arch Neurol 2006; 63(1): 81-6.

Braak H, Alafuzoff I, Arzberger T, Kretzschmar H, Del Tredici K. Staging of Alzheimer disease-associated neurofibrillary pathology using paraffin sections and immunocytochemistry. Acta Neuropathol 2006; 112(4): 389-404.

Braak H, Del Tredici K, Rub U, de Vos RA, Jansen Steur EN, Braak E. Staging of brain pathology related to sporadic Parkinson's disease. Neurobiol Aging 2003; 24(2): 197-211.

Braak H, Thal DR, Ghebremedhin E, Del Tredici K. Stages of the pathologic process in Alzheimer disease: age categories from 1 to 100 years. J Neuropathol Exp Neurol 2011; 70(11): 960-9.

Brettschneider J, Del Tredici K, Irwin DJ, Grossman M, Robinson JL, Toledo JB, *et al.* Sequential distribution of pTDP-43 pathology in behavioral variant frontotemporal dementia (bvFTD). Acta Neuropathol 2014; 127(3): 423-39.

Brettschneider J, Del Tredici K, Toledo JB, Robinson JL, Irwin DJ, Grossman M, *et al.* Stages of pTDP-43 pathology in amyotrophic lateral sclerosis. Ann Neurol 2013; 74(1): 20-38.

Clavaguera F, Akatsu H, Fraser G, Crowther RA, Frank S, Hench J, *et al.* Brain homogenates from human tauopathies induce tau inclusions in mouse brain. Proc Natl Acad Sci U S A 2013; 110(23): 9535-40.

Clavaguera F, Bolmont T, Crowther RA, Abramowski D, Frank S, Probst A, *et al.* Transmission and spreading of tauopathy in transgenic mouse brain. Nat Cell Biol 2009; 11(7): 909-13.

Dickson DW, Bergeron C, Chin SS, Duyckaerts C, Horoupian D, Ikeda K, *et al.* Office of Rare Diseases neuropathologic criteria for corticobasal degeneration. J Neuropathol Exp Neurol 2002; 61(11): 935-46.

Dickson DW, Fujishiro H, DelleDonne A, Menke J, Ahmed Z, Klos KJ, *et al.* Evidence that incidental Lewy body disease is pre-symptomatic Parkinson's disease. Acta Neuropathol 2008; 115(4): 437-44.

Evidente VG, Adler CH, Sabbagh MN, Connor DJ, Hentz JG, Caviness JN, *et al.* Neuropathological findings of PSP in the elderly without clinical PSP: possible incidental PSP? Parkinsonism Relat Disord 2011; 17(5): 365-71.

Fearnley JM, Lees AJ. Ageing and Parkinson's disease: substantia nigra regional selectivity. Brain 1991; 114 (Pt 5): 2283-301.

Frigerio R, Fujishiro H, Ahn TB, Josephs KA, Maraganore DM, DelleDonne A, *et al.* Incidental Lewy body disease: do some cases represent a preclinical stage of dementia with Lewy bodies? Neurobiol Aging 2011; 32(5): 857-63.

Fujishiro H, Ahn TB, Frigerio R, DelleDonne A, Josephs KA, Parisi JE, *et al.* Glial cytoplasmic inclusions in neurologically normal elderly: prodromal multiple system atrophy? Acta Neuropathol 2008; 116(3): 269-75.

Gundersen HJ, Bendtsen TF, Korbo L, Marcussen N, Moller A, Nielsen K, *et al.* Some new, simple and efficient stereological methods and their use in pathological research and diagnosis. APMIS 1988; 96(5): 379-94.

Halliday G, Hely M, Reid W, Morris J. The progression of pathology in longitudinally followed patients with Parkinson's disease. Acta Neuropathol 2008; 115(4): 409-15.

Hassan A, Whitwell JL, Boeve BF, Jack CR, Jr., Parisi JE, Dickson DW, *et al.* Symmetric corticobasal degeneration (S-CBD). Parkinsonism Relat Disord 2010; 16(3): 208-14.

Hauw JJ, Daniel SE, Dickson D, Horoupian DS, Jellinger K, Lantos PL, *et al.* Preliminary NINDS neuropathologic criteria for Steele-Richardson-Olszewski syndrome (progressive supranuclear palsy). Neurology 1994; 44(11): 2015-9.

Houlden H, Baker M, Morris HR, MacDonald N, Pickering-Brown S, Adamson J, *et al.* Corticobasal degeneration and progressive supranuclear palsy share a common tau haplotype. Neurology 2001; 56(12): 1702-6.

Hyman BT, Phelps CH, Beach TG, Bigio EH, Cairns NJ, Carrillo MC, *et al.* National Institute on Aging-Alzheimer's Association guidelines for the neuropathologic assessment of Alzheimer's disease. Alzheimer's & dementia : the journal of the Alzheimer's Association 2012; 8(1): 1-13.

Irwin DJ, Brettschneider J, McMillan CT, Cooper F, Olm C, Arnold SE, *et al.* Deep clinical and neuropathological phenotyping of Pick disease. Ann Neurol 2016; 79(2): 272-87.

Josephs KA, Mandrekar JN, Dickson DW. The relationship between histopathological features of progressive supranuclear palsy and disease duration. Parkinsonism Relat Disord 2006; 12(2): 109-12.

Kouri N, Whitwell JL, Josephs KA, Rademakers R, Dickson DW. Corticobasal degeneration: a pathologically distinct 4R tauopathy. Nat Rev Neurol 2011; 7(5): 263-72.

Lewis J, Dickson DW. Propagation of tau pathology: hypotheses, discoveries, and yet unresolved questions from experimental and human brain studies. Acta Neuropathol 2016; 131(1): 27-48.

Ling H, de Silva R, Massey LA, Courtney R, Hondhamuni G, Bajaj N, *et al.* Characteristics of progressive supranuclear palsy presenting with corticobasal syndrome: a cortical variant. Neuropathology and applied neurobiology 2013.

Ling H, O'Sullivan SS, Holton JL, Revesz T, Massey LA, Williams DR, *et al.* Does corticobasal degeneration exist? A clinicopathological re-evaluation. Brain 2010; 133(Pt 7): 2045-57.

McKee AC, Stein TD, Nowinski CJ, Stern RA, Daneshvar DH, Alvarez VE, *et al.* The spectrum of disease in chronic traumatic encephalopathy. Brain : a journal of neurology 2013; 136(Pt 1): 43-64.

Milenkovic I, Kovacs GG. Incidental corticobasal degeneration in a 76-year-old woman. Clin Neuropathol 2013; 32(1): 69-72.

Niethammer M, Tang CC, Feigin A, Allen PJ, Heinen L, Hellwig S, *et al.* A disease-specific metabolic brain network associated with corticobasal degeneration. Brain 2014; 137(Pt 11): 3036-46.

Nishida N, Yoshida K, Hata Y, Arai Y, Kinoshita K. Pathological features of preclinical or early clinical stages of corticobasal degeneration: a comparison with advanced cases. Neuropathol Appl Neurobiol 2015; 41(7): 893-905.

O'Sullivan SS, Burn DJ, Holton JL, Lees AJ. Normal dopamine transporter single photon-emission CT scan in corticobasal degeneration. Mov Disord 2008; 23(16): 2424-6.

Oide T, Ohara S, Yazawa M, Inoue K, Itoh N, Tokuda T, *et al.* Progressive supranuclear palsy with asymmetric tau pathology presenting with unilateral limb dystonia. Acta Neuropathol 2002; 104(2): 209-14.

Oshima K, Tsuchiya K, Iritani S, Niizato K, Akiyama H, Arai H, *et al.* [An autopsy case of "progressive supranuclear palsy" without psychiatric or neurological signs]. No To Shinkei 2004; 56(2): 157-61.

Parkkinen L, Hartikainen P, Alafuzoff I. Abundant glial alpha-synuclein pathology in a case without overt clinical symptoms. Clin Neuropathol 2007; 26(6): 276-83.

Piattella MC, Tona F, Bologna M, Sbardella E, Formica A, Petsas N, *et al.* Disrupted resting-state functional connectivity in progressive supranuclear palsy. AJNR Am J Neuroradiol 2015; 36(5): 915-21.

Pirker S, Perju-Dumbrava L, Kovacs GG, Traub-Weidinger T, Pirker W. Progressive Dopamine Transporter Binding Loss in Autopsy-Confirmed Corticobasal Degeneration. J Parkinsons Dis 2015; 5(4): 907-12.

Pittman AM, Myers AJ, Abou-Sleiman P, Fung HC, Kaleem M, Marlowe L, *et al.* Linkage disequilibrium fine mapping and haplotype association analysis of the tau gene in progressive supranuclear palsy and corticobasal degeneration. J Med Genet 2005; 42(11): 837-46.

Rebeiz JJ, Kolodny EH, Richardson EP, Jr. Corticodentatonigral degeneration with neuronal achromasia: a progressive disorder of late adult life. Trans Am Neurol Assoc 1967; 92: 23-6.

Rebeiz JJ, Kolodny EH, Richardson EP, Jr. Corticodentatonigral degeneration with neuronal achromasia. Arch Neurol 1968; 18(1): 20-33.

Rinne JO, Rummukainen J, Paljarvi L, Rinne UK. Dementia in Parkinson's disease is related to neuronal loss in the medial substantia nigra. Ann Neurol 1989; 26(1): 47-50.

Saito Y, Ruberu NN, Sawabe M, Arai T, Tanaka N, Kakuta Y, *et al.* Staging of argyrophilic grains: an age-associated tauopathy. J Neuropathol Exp Neurol 2004; 63(9): 911-8.

Togo T, Sahara N, Yen SH, Cookson N, Ishizawa T, Hutton M, *et al.* Argyrophilic grain disease is a sporadic 4-repeat tauopathy. J Neuropathol Exp Neurol 2002; 61(6): 547-56.

Whitwell JL, Jack CR, Jr., Boeve BF, Parisi JE, Ahlskog JE, Drubach DA, *et al.* Imaging correlates of pathology in corticobasal syndrome. Neurology 2010; 75(21): 1879-87.

Whitwell JL, Josephs KA. Recent advances in the imaging of frontotemporal dementia. Curr Neurol Neurosci Rep 2012; 12(6): 715-23.

Williams DR, de Silva R, Paviour DC, Pittman A, Watt HC, Kilford L*, et al.* Characteristics of two distinct clinical phenotypes in pathologically proven progressive supranuclear palsy: Richardson's syndrome and PSP-parkinsonism. Brain 2005; 128(Pt 6): 1247-58.

Table 1: Characteristics and secondary pathologies of preclinical CBD (Cases 1-3) and end-stage CBD (Cases 4-9) cases.

Case No.	Gender	Clinical diagnosis	Age at death (years)	Disease duration from symptom onset (years)	Clinically more affected side	Whole brain weight	Hemisphere examined*	NIA-AA score (Level of AD neuropathological change)(Hyman *et al*., 2012)	TDP-43 proteinopathy	Argyrophilic grains(Saito *et al*., 2004)	C9Orf72 inclusions**	α-synuclein pathology	Vascular pathology	CAA
Case 1 (Preclinical, QSBB)	Male	Tourette's Syndrome	63	NA	NA	1441g	Left	A0, B1, C0 (Not)	-	-	-	-	-	-
Case 2 (Preclinical, New York)	Male	US Aging Project	89	NA	NA	1315g	Right	A1, B0, C0 (Low)	-	-	-	-	-	-
Case 3 (Preclinical, Vienna)	Female	Kidney Transplant	76	NA	NA	1120g	Left	A0, B1, C0 (Not)	-	Yes	-	-	-	-
Case 4 (End-stage CBD-CBS)	Male	CBS	78	8	Right	1216g	Right	A1, B1, C1 (Low)	-	-	-	-	-	-
Case 5 (End-stage CBD-CBS)	Male	CBS	72	5	Left	1378g	Left	A0, B2, C0 (Not)	-	-	-	-	Mild SVD	-
Case 6 (End-stage CBD-CBS)	Male	CBS	73	7	Left	1154g	Left	A0, B1, C0 (Not)	-	-	-	-	Mild SVD	-
Case 7 (End-stage CBD-RS)	Female	RS	68	5	NA	1034g	Left	A1, B1, C1 (Low)	Limbic	Yes	-	-	-	-
Case 8 (End-stage CBD-RS)	Male	RS	64	4	NA	1210g	Left	A1, B1, C1 (Low)	Limbic	Yes	-	-	Mild SVD	-
Case 9 (End-stage CBD-RS)	Male	RS	66	4	NA	1200g	Right	A1, B1, C1 (Low)	Limbic	Yes	-	-	-	Mild

AD: Alzheimer's disease, CAA: cerebral amyloid angiopathy, CBD: corticobasal degeneration, CBS: corticobasal syndrome, NA: not applicable, NK: not known, QSBB: Queen Square Brain Bank for Neurological Disorders, London, UK, RS: Richardson syndrome, US: United States, SVD: small vessel disease; *hemisphere examined was randomly selected, **screening for inclusions using p62 immunohistochemistry in hippocampus and cerebellum, -: negative/absent.

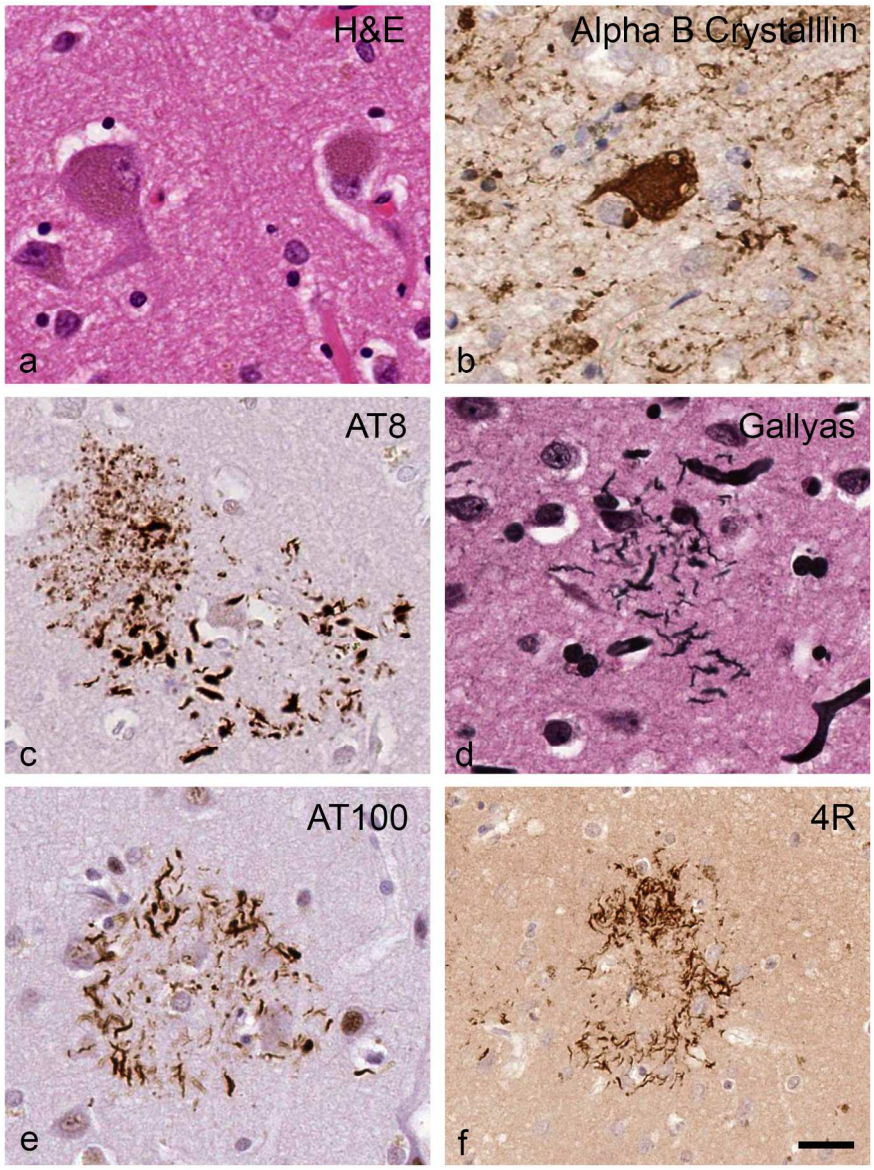

Ballooned neurons (a & b; end-stage CBD Case 6) and astrocytic plaques (c-f; preclinical CBD Case 1). Ballooned neuron is absent in Cases 1 and 2. Occasional ballooned neurons observed in the cingulate cortex in Case 3 are probably associated with the coexisting argyrophilic grain disease rather than CBD pathology. Astrocytic plaque is a prominent histological finding in preclinical CBD cases, especially in the anterior frontal cortex (c-f) and caudate, and is immunoreactive for AT8 (c), AT100 (e) and 4-repeat tau (f), but not 3-repeat tau, and is Gallyas-positive (d). 1 cm scale bar = 10 μm.

Fig. 1

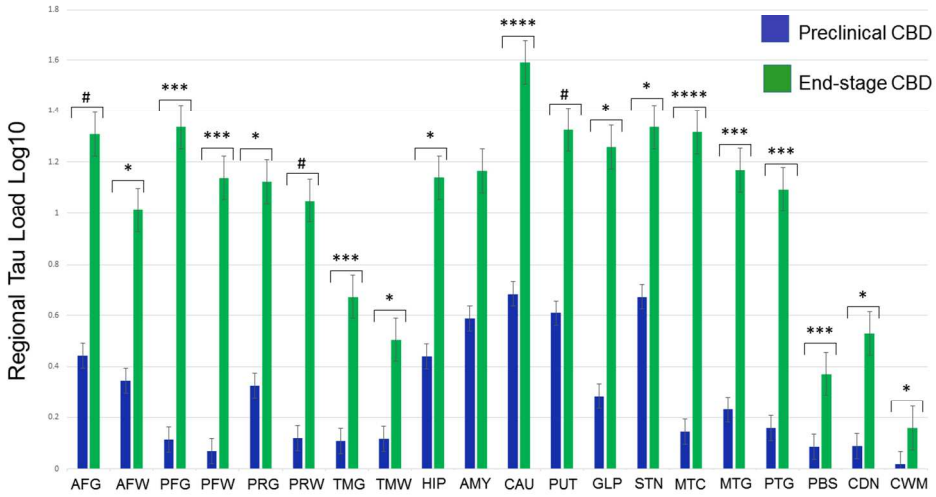

Mean regional tau load (Log10) of preclinical CBD and end-stage CBD groups in 20 selected brain regions. Error bars represent one standard error of the mean (SEM). ****P value < 0.001, ***P value: 0.001-0.005, **P value: 0.005-0.01, *P value: 0.01-0.05, #P value: 0.05-0.01 (borderline statistical significance), Student's t-test; AFG: anterior frontal grey matter, AFW: anterior frontal white matter, PFG: posterior frontal grey matter, PFW: posterior frontal white matter, PRG: parietal grey matter, PR: parietal white matter, TMG: temporal grey matter, TMW: temporal white matter, HIP: hippocampus, AMG: amygdala, CAU: caudate, PUT: putamen, GLP: globus pallidus, STN: subthalamic nucleus, MTC: midbrain tectum, MTG: midbrain tegmentum, PTG: pontine tegmentum, PBS: pontine base, CDN: cerebellar dentate nucleus and CWM: cerebellar white matter.

Fig. 2
370x250mm (96 x 96 DPI)

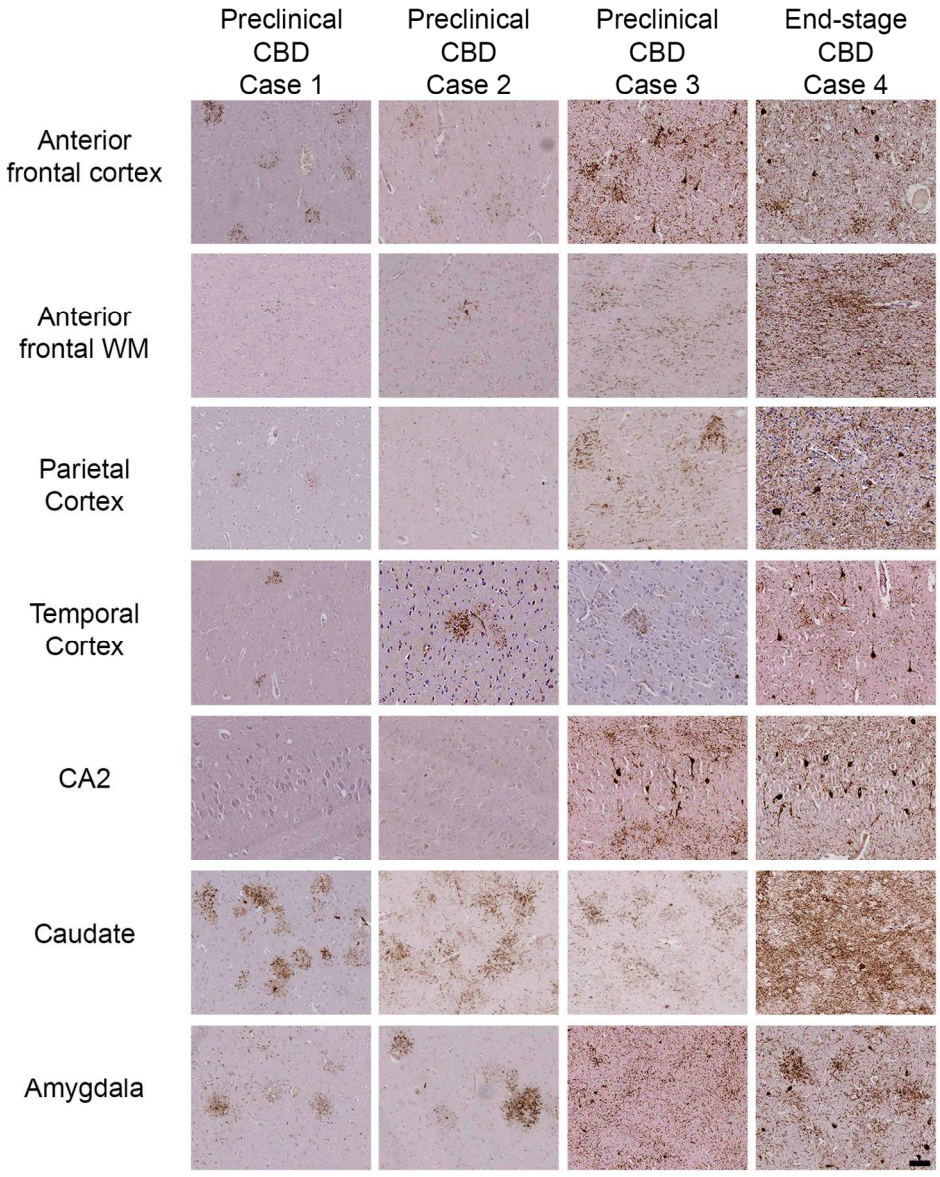

Tau immunohistochemistry (AT8) sections of the three preclinical CBD cases (Cases 1-3) and one end-stage CBD-CBS case (Case 4). 1 cm scale bar = 38.5 μm.
Fig. 3

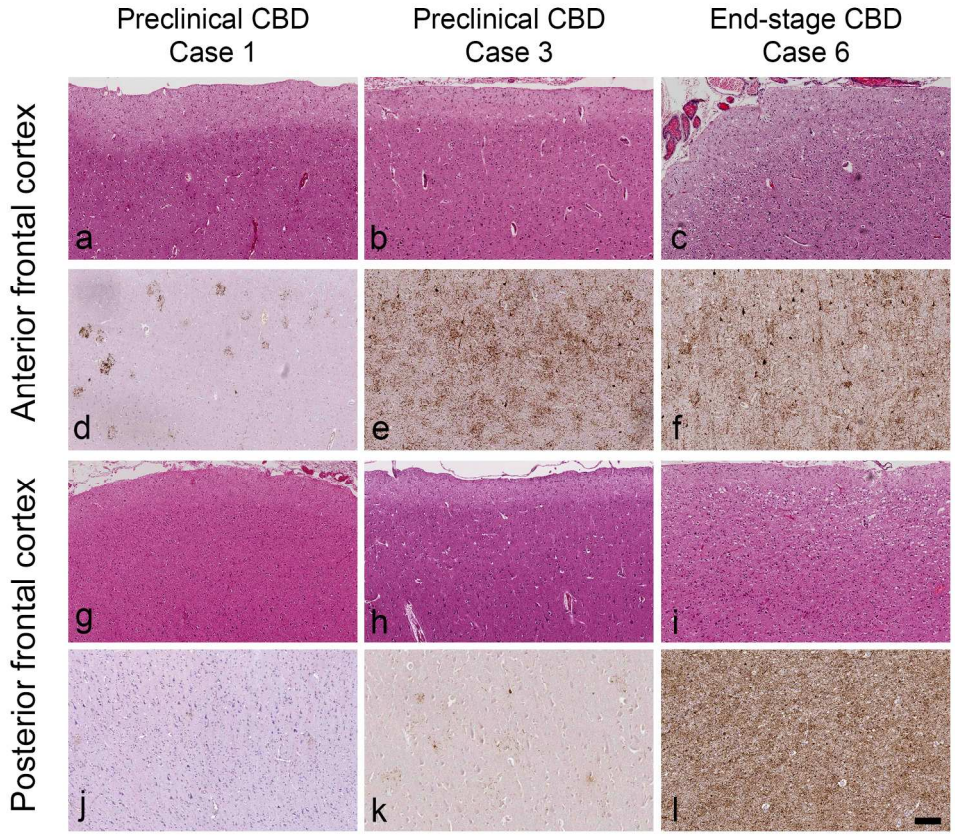

Anterior and posterior frontal cortex of two preclinical CBD (Cases 1 and 3) and one end-stage CBD-CBS case (Case 6). ‼ ┼ The characteristic features of cortical neuronal loss and superficial spongiosis are observed in the end-stage CBD case (c & i) but not in the preclinical CBD cases (a, b & g, h). In the preclinical CBD cases, tau immunohistochemistry (AT8) demonstrates tau lesions, mainly in the form of astrocytic plaques, are more abundant in the anterior frontal cortex (d & e) than in the posterior frontal cortex (j & k). This anterior-posterior gradient is most apparent in Case 1 (d & j), which has a relatively less total tau load and is thought to represent an earlier stage of CBD pathology than Case 3. On the contrary, in the end-stage CBD case, neurofibrillary tangles and neuropil threads are much more frequent than astrocytic plaques and the tau distribution is more severe in the posterior frontal cortex (l) than in the anterior frontal cortex (f). H&E: a-c, g-i; tau immunohistochemistry (AT8): d-f, j-l; 1 cm scale bar = 100μm.‼ ┼

Fig. 4

199x178mm (300 x 300 DPI)

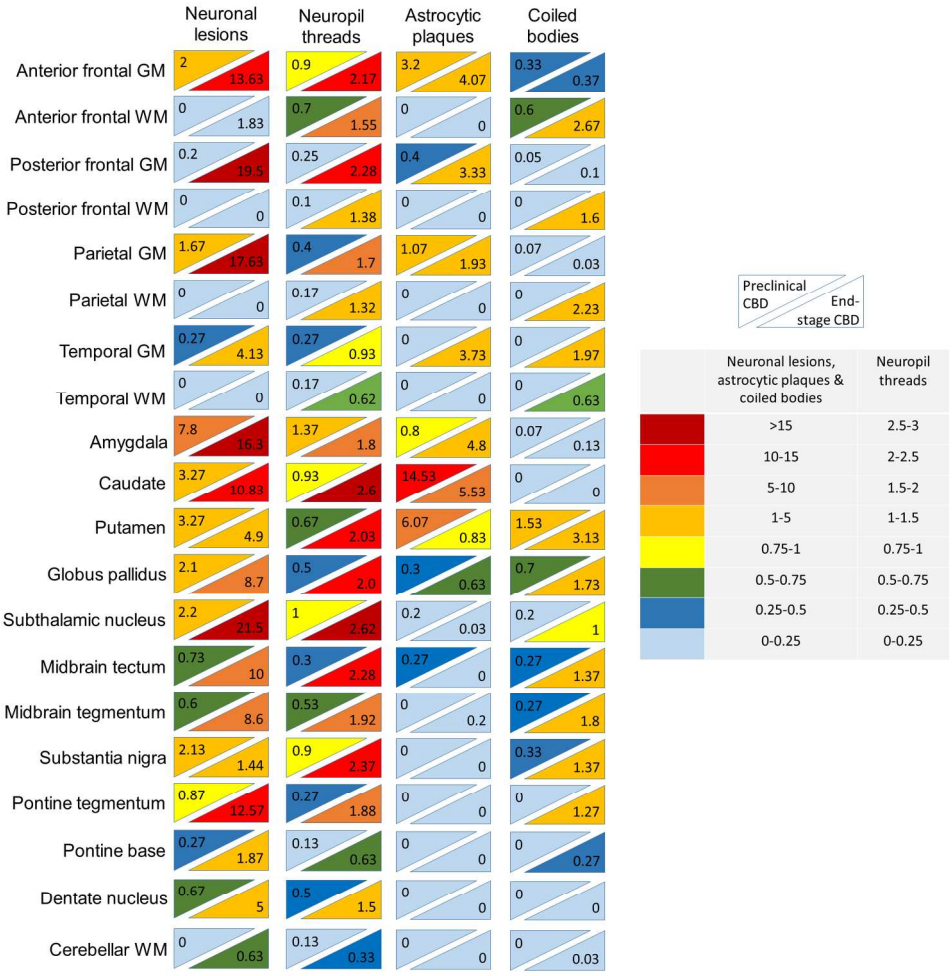

Distribution and severity of tau-immunoreactive cellular lesions in preclinical and end-stage CBD groups. ‼ ┼ A summary of the tau pathology in 3 preclinical CBD and 6 end-stage CBD (3 CBD-CBS and 3 CBD-RS) cases using mean lesion count for neuronal lesions, astrocytic plaques and coiled bodies and a 4-tier semi-quantitative scores for neuropil thread (0 = none, 1 = mild, 2 = moderate, 3 = severe) assessed at x20 objective in 5 random fields (except for substantia nigra, subthalamic and dentate nuclei where 3 random fields were used due to small regional areas). The severity of tau pathology is colour-coded with a heat map, with more severely affected areas showing hotter colours (red, orange and yellow) and less affected areas represented by cooler colours (green and blue).‼ ┼

Fig. 5

550x550mm (96 x 96 DPI)

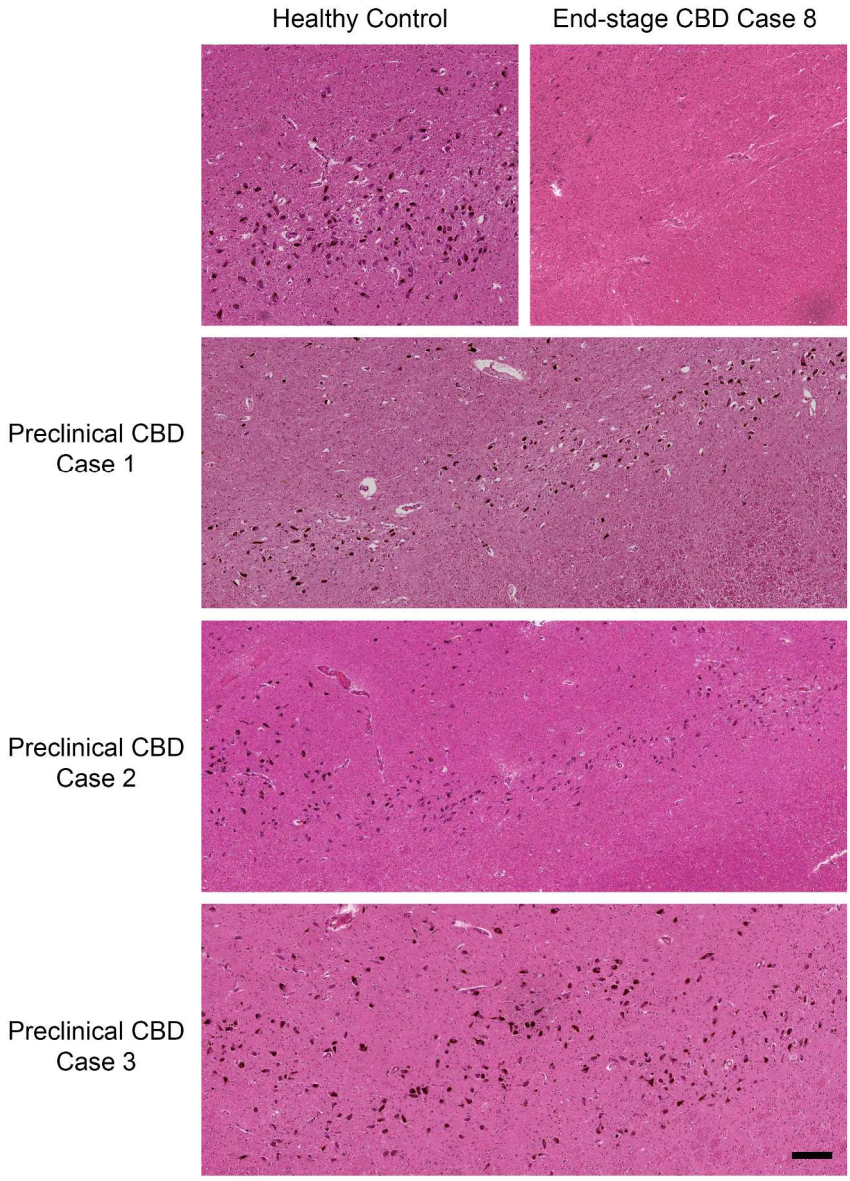

H&E sections of the substanti nigra.├ ┬ The substantia nigra of the three preclinical CBD Cases 1-3 and an 82-year-old healthy control are relatively preserved with a good population of pigmented neurons. Severe loss of pigmented neurons, gliosis and scaring are observed in the substantia nigra of the end-stage CBD-RS Case 8. 1 cm scale bar = 100 μm.├ ┬
Fig. 6

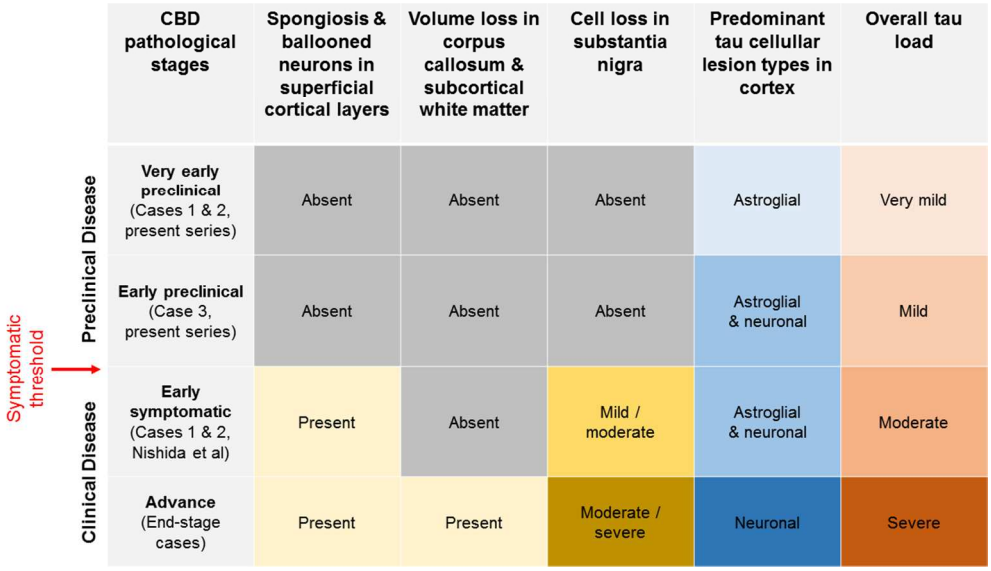

CBD pathological stages	Spongiosis & ballooned neurons in superficial cortical layers	Volume loss in corpus callosum & subcortical white matter	Cell loss in substantia nigra	Predominant tau cellular lesion types in cortex	Overall tau load
Very early preclinical (Cases 1 & 2, present series)	Absent	Absent	Absent	Astroglial	Very mild
Early preclinical (Case 3, present series)	Absent	Absent	Absent	Astroglial & neuronal	Mild
Early symptomatic (Cases 1 & 2, Nishida et al)	Present	Absent	Mild / moderate	Astroglial & neuronal	Moderate
Advance (End-stage cases)	Present	Present	Moderate / severe	Neuronal	Severe

Characteristic features of the pathological progression of CBD.
Fig. 7
338x190mm (96 x 96 DPI)

SUPPLEMENTARY MATERIALS

Supplementary Fig. 1:

Regional tau load determined by measuring all tau immunoreactive lesions by image analysis in each preclinical case (Cases 1 to 3; data provided in brackets). Only selected brain regions are illustrated. In Case 3, tissue sections of the posterior frontal region and subthalamic nucleus were not available for analysis. GM: grey matter, WM: white matter.

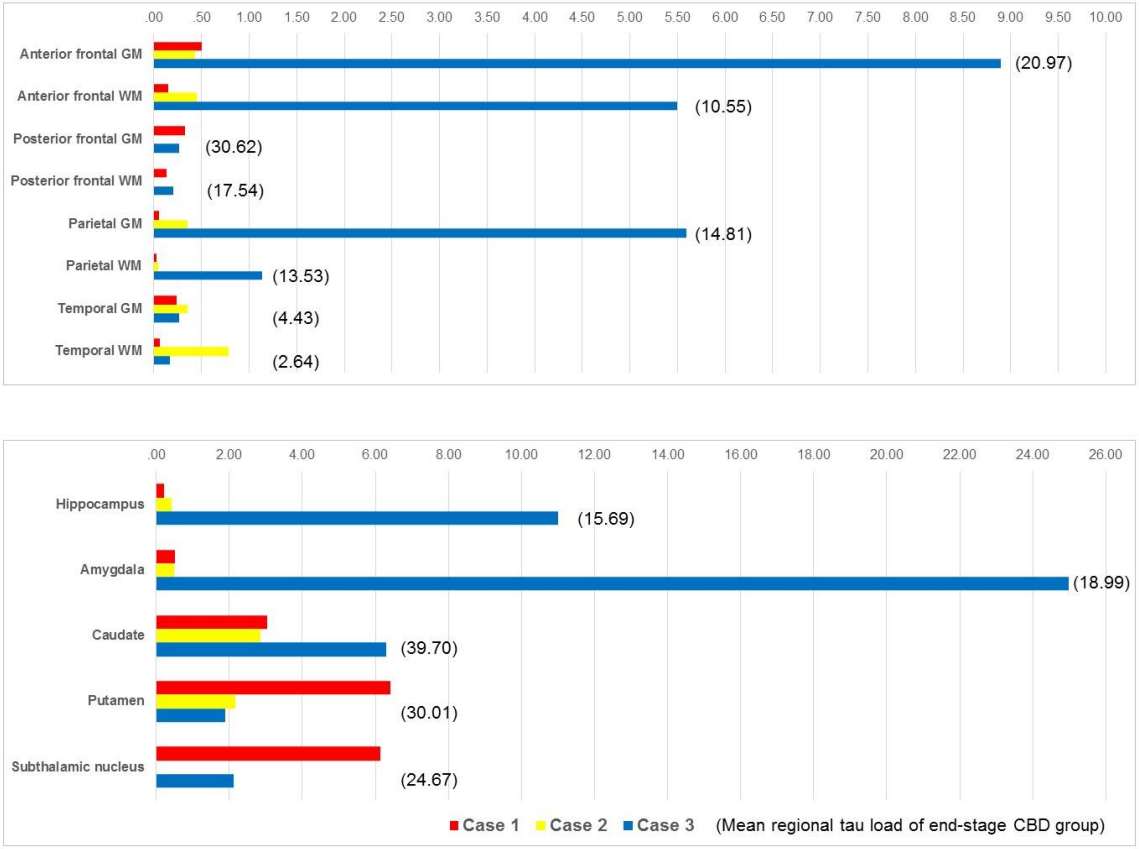

Supplementary Fig. 2:

Mean total, cortical and basal ganglia tau load of preclinical CBD and end-stage CBD groups.

Error bars represent one standard error of the mean (SEM). ***P value: 0.001-0.005, *P value: 0.01-0.05, #P value: 0.05-0.01 (borderline statistical significance), Student's t-test; BG: basal ganglia.

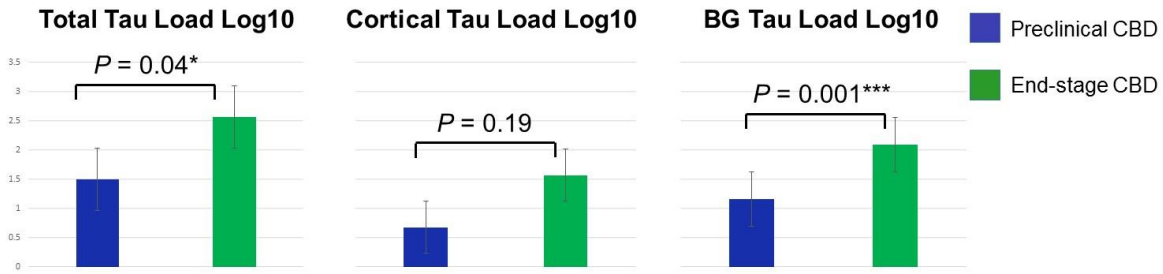

Supplementary Fig. 3:

Tau pathology in the cortical regions of the preclinical and end-stage CBD groups.

Mean lesion count for neuronal lesions, astrocytic plaques and coiled bodies and a 4-tier semi-quantitative grading scores for neuropil thread were assessed at x20 objective in 5 random fields in the anterior and posterior frontal, parietal and temporal grey matter and white matter. Supplementary Fig 3 illustrates the mean count of neuronal lesions and astrocytic plaques in the two groups. Error bars represent one standard error of the mean (SEM).

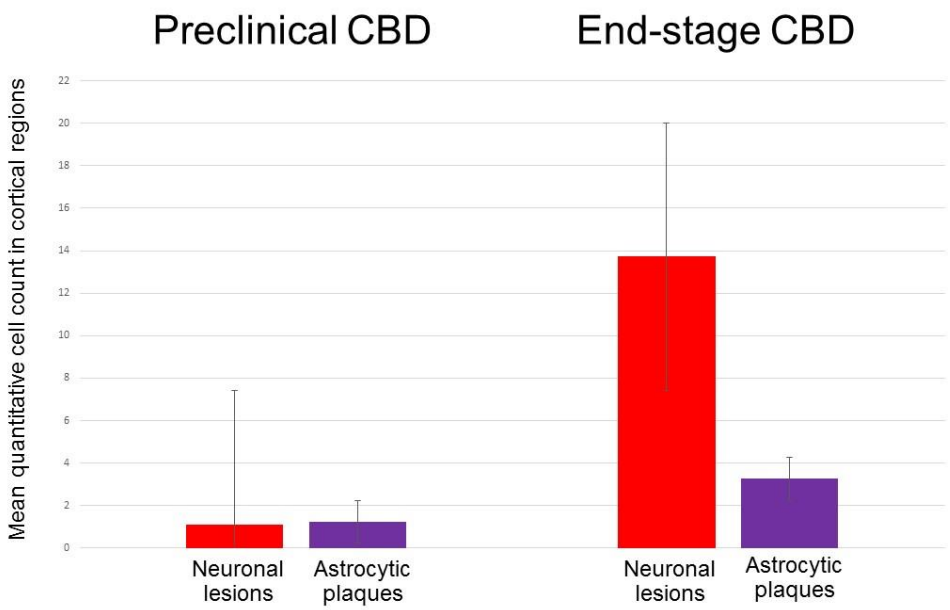

Supplementary Fig. 4:

Correlations between lesion types and tau load in the cortical regions. In preclinical CBD cases, significant correlation was found between neuronal lesions and regional tau load (Pearson correlation coefficient = 0.95). In end-stage CBD, significant correlation was found between thread pathology and regional tau load (Pearson correlation coefficient = 0.86). Regions included in the analysis were anterior and posterior frontal, parietal and temporal grey matter and white matter.

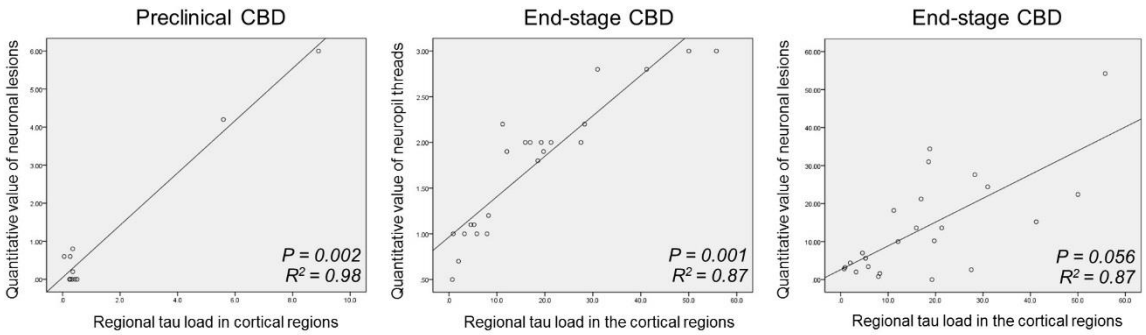

Supplementary Fig. 5:

Tau-immunoreactive neuronal and thread lesions in the hippocampal subregions of preclinical and end-stage CBD cases. A 4-tier semi-quantitative grading scheme was used: 0 = none, 1 = mild, 2 = moderate, 3 = severe. AD: Alzheimer's disease, EC: entorhinal cortex, GCL: granular cell layer, NFT: neurofibrillary tangle, PreT: pretangle. NIA-AA ABC score (Hyman *et al.*, 2012), argyrophilic grains (Saito *et al.*, 2004).

	Preclinical CBD						End-stage CBD									
	Case 1		Case 2		Case 3		Case 4		Case 5		Case 6		Case 7		Case 8		Case 9	
ABC Score (Level of AD neuropathological change)[1]	A0, B1, C0 (Not)		A1, B0, C0 (Low)		A0, B1, C0 (Not)		A1, B1, C1 (Low)		A0, B2, C0 (Not)		A0, B1, C0 (Not)		A1, B1, C1 (Low)		A1, B1, C1 (Low)		A1, B1, C1 (Low)	
Argyrophilic grains [2]	–		–		YES		–		–		–		YES		YES		YES	
Hippcampal subregions	NFT/ PreT	NT	NFT/ PreT	NT	NFT/ PreT	NT	NFT/ PreT	NT	NFT/ PreT	NT	NFT/ PreT	NT	NFT/ PreT	NT	NFT/ PreT	NT	NFT/ PreT	NT
CA1	0	1	1	1	3	3	2	2	1	1	3	3	2	2	2	3	2	2
CA2	0.5	0	1	1	2	2	2	2	0	0.5	2	1	2	2	2	2	2	2
CA3	0	0	1	1	1	1	2	2	0	0.5	2	1	1	1	1	1	1	1
CA4	0	0	1	1	1	1	2	2	0.5	0.5	1	1	1	1	1	2	1	1
GCL	0	1	0.5	0	3	0	3	2	1	1	3	1	3	1	3	2	2	1
Subiculum	1	1	1	1	3	3	3	3	2	2	2	2	2	3	2	3	1	3
EC	1	1	0	1	1	0	2	2	1	1	2	2	2	2	2	2	0.5	2

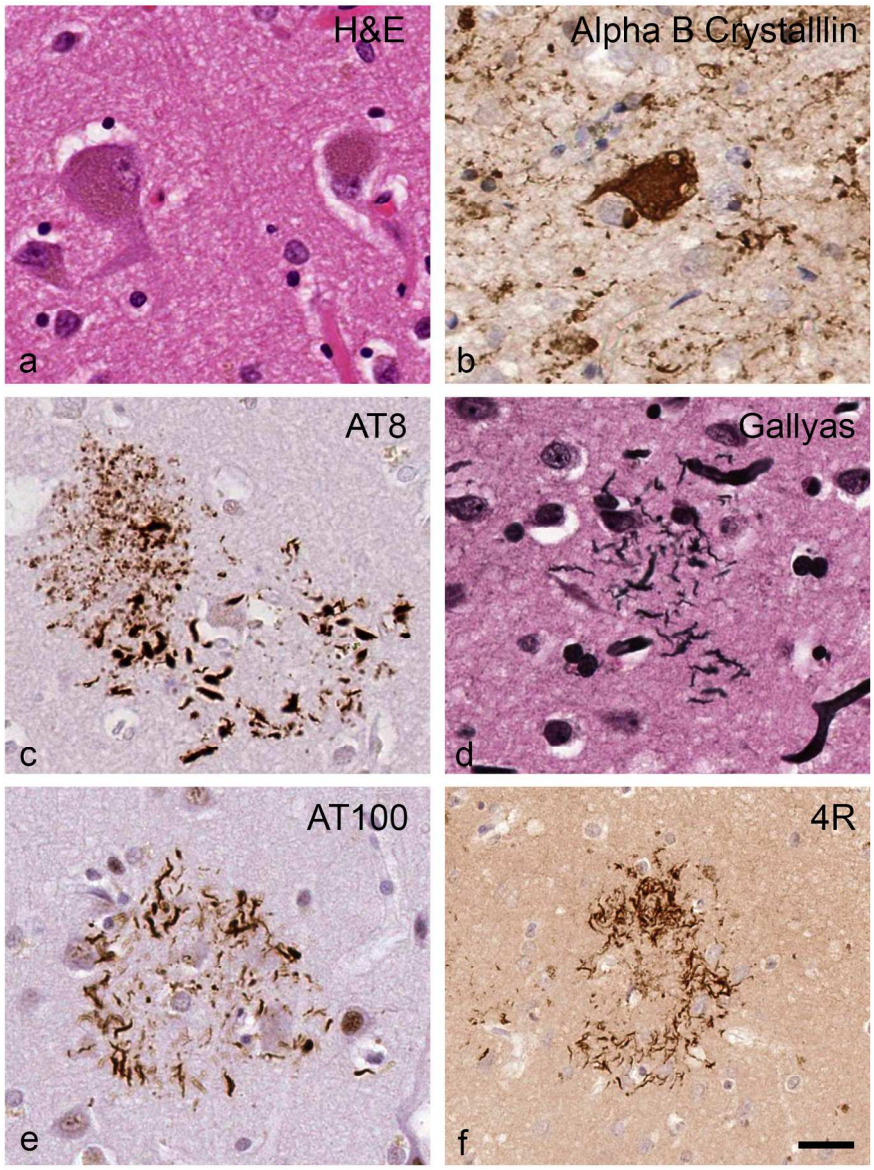
H&E
a
Alpha B Crystalllin
b
AT8
c
Gallyas
d
AT100
e
4R
f